Supplementary data

Title:

Dendritic Cell-Based Immunotherapy in Prevention and Treatment of Renal Cell Carcinoma: Efficacy, Safety, and Anti-tumor Activity of Ad-GM·CAIX in Immunocompetent Mouse Models.

Authors:

Frédéric D Birkhäuser, Richard C Koya, Caleb Neufeld, Edward N Rampersaud, Xuyang Lu, Ewa D Micewicz, Thinle Chodon, Mohammad Atefi, Nils Kroeger, Gadisetti VR Chandramouli, Gang Li, Jonathan W Said, William H McBride, Fairooz F Kabbinavar, Antoni Ribas, Allan J Pantuck, Arie S Belldegrun§, Joseph Riss§

Methods

Cells and cell culture. RENCA is a spontaneous murine renal cortical adenocarcinoma arising in Balb/c mice and is a model of human adult RCC in immunocompetent syngeneic mice (Balb/c) (1). RENCA cells were a gift from Dr. R. Wiltrout (NCI/NIH) (2). RENCA-CAIX cells were generated by stably transducing the human CAIX gene in RENCA cells (3). NPR-IX cells are hCAIX FACS-purified RENCA-CAIX cells, which repeatedly had >90% hCAIX-positive cells in flow cytometry analysis (**Supplementary Fig. S2**). All cells were cultured in RPMI-1640 medium (Life Technologies, NY) supplemented with 10% FBS (Life Technologies), 1% Pen-Strep (Omega Scientific, CA), 1% MEM non-essential amino acids solution (Life Technologies), and 1% sodium pyruvate (Life Technologies).

***In vitro* DC generation and gene transduction.** Bone marrow cells of 8-week-old female Balb/c mice were induced to differentiate into DCs as described previously by Koya et al (4). The differentiated DCs (2.5x10^6 cells/ml) were cultured in RPMI supplemented with 10% FBS, 1% Pen-Strep, 50 ng/ml mGM-CSF, and 50 ng/ml mIL-4. Half were infected with Ad-GM·CAIX (5) (**Supplementary Fig. S3**) and half with an empty adenoviral capsid identical to Ad-GM·CAIX's (Ad-Null; Welgen, MA), each at a multiplicity of infection of 200. After an overnight incubation, the infected DCs were washed with and re-suspended in PBS 1x (1.33x10^7 cells/ml). Using intracellular and extracellular FACS analysis, the expression levels of Cd11c (not shown), Cd86, hCAIX, and hGM-CSF were used to test for DC differentiation and GM·CAIX transduction (**Supplementary Fig. S4 and S5**).

Western blot. Rabbit α-hCAIX (Pierce, IL), mouse α-hGM-CSF (Pierce, IL), rabbit α-actin cell signaling, goat α-rabbit IgG-HRP (Santa Cruz, CA), and goat α-mouse IgG-HRP

(Santa Cruz, CA) antibodies were used. Chemiluminescence was elicited using the Amersham ECL-Plus (GE Healthcare, NJ) western blotting detection system.

Immunohistochemistry. In three mice of each group of the prevention model, pathology-relevant organs, blood, and tumors were collected. Paraffin-embedded sections were cut at 4 µm thickness and rehydrated through graded ethanol. Endogenous peroxidase activity was blocked with 3% hydrogen peroxide in methanol for 10 min. Heat-induced antigen retrieval and proteolytic induced epitope retrieval were used. The slides were then stained with hCAIX (rabbit, 1:1000 dilution, Novus Biological, CO), mCAIX (goat, 1:200, R&D System, MN), Ki67 (rat, 1:100, DAKO, CA), Pecam1 (Cd31) (goat, 1:100, Santa Cruz, CA), Cd11b (rat, 1:50, AbDSerotec, NC), and F4/80 (rat, 1:50, AbDSerotec), and the sections were incubated with secondary rabbit and rat (Cd11b, F4/80, Ki67) or rabbit anti-goat (Cd31, mCAIX) immunoglobulin for 30 min at 1:200 dilution (DakoCytomation). The signal was detected using the Dakocytomation Envision System Labelled Polymer HRP anti rabbit (DakoCytomation) for all. For Tunel assays, an ApoptagPlus Peroxidase In Situ Apoptosis kit (Millipore, MA) was used. Staining was performed according to the manufacturer's instructions. All sections were visualized with the diaminobenzidine reaction and counterstained with hematoxylin.

Gene expression analysis. The gene expression was investigated by Agilent 60-mer oligonucleotide probe arrays (SurePrint G3 Mouse GE 8x60K, Agilent, CA), using the highest absolute value/score among multiple probe sets for the gene-based interpretation. Background corrected signal values determined by Agilent feature extraction software were normalized by median centering of the ratios to a reference, which is the median of all control arrays. The features called *found* by extraction software were considered as present or detected. Global expression profiles of samples were examined by

multidimensional scaling of about 36,000 features that were found at least in 50% of the arrays. Euclidean distance was used as the dissimilarity measure. The features having presence calls in <80% of samples and a geometric mean signal <50 in both groups A and C were eliminated before further analyses. In those remaining, there were 367 mRNA features differentially expressed by 1.5-fold (two tailed p-value < 0.015 by T-test). Ingenuity pathway analyses were done on the datasets of differentially expressed genes (P<0.05). Publicly available literature from 1966 to 2012 was surveyed using CoreMine and PubMed.

miRNA expression analysis. ExiqonmiRNA arrays (miRCURY LNA™ microRNA array, v6, Exiqon, Denmark) having more than 1,891 capture probes covering all human, mouse, rat, and viral miRNAs and 66 proprietary miRNAs spotted in quadruplicate were used for measuring genome miRNA expression. Intensities were determined by GenePix Pro 6.0 software (Molecular Devices, Sunnyvale, CA) and were normalized by median centering of the ratios to a reference control array. Global miRNA expression profiles of samples were examined by multidimensional scaling of about 4,200 features that were flagged as found in ≥50% of the samples. The features found in <60% of samples in both groups A and C were eliminated from further analysis. There were 104 miRNAs differentially expressed by 1.5-fold (two tailed p-value < 0.015 by T-test), and 11 mouse miRNA replicates appeared 50-100% of the time at signal levels ≥200.

References

1. Murphy GP, Hrushesky WJ. A murine renal cell carcinoma. J Natl Cancer Inst. 1973;50:1013-25.

2. Wiltrout RH, Gregorio TA, Fenton RG, et al. Cellular and molecular studies in the treatment of murine renal cancer. Semin Oncol. 1995;22:9-16.

3. Shvarts O, Janzen N, Lam JS, et al. RENCA/carbonic anhydrase-IX: a murine model of a carbonic anhydrase-IX-expressing renal cell carcinoma. Urology. 2006;68:1132-8.

4. Koya RC, Kimura T, Ribas A, et al. Lentiviral vector-mediated autonomous differentiation of mouse bone marrow cells into immunologically potent dendritic cell vaccines. Mol Ther. 2007;15:971-80.

5. Hernandez JM, Bui MH, Han KR, et al. Novel kidney cancer immunotherapy based on the granulocyte-macrophage colony-stimulating factor and carbonic anhydrase IX fusion gene. Clin Cancer Res. 2003;9:1906-16.

Tables and Figures

Supplementary Table S1. File “Suppl._File_EXPRESSION.xlsx”

Supplementary Table S2. Differentially expressed genes in the tumors that evaded DC-Ad-GM·CAIX immunotherapy versus DC-Ad-Null. (a) Genes in the ontology category “Inflammatory Response.” (b) Genes in the ontology category “Cellular Growth and Proliferation.”

(**A**) Gene ontology category: Inflammatory Response

Functions annotation	**p-Value**	**Molecules**
Tethering of dendritic cells	1.01E-04	CD209,ICAM2
Adhesion of dendritic cells	2.69E-04	CD209,ICAM1,ICAM2
Transmigration of dendritic cells	3.40E-04	CD209,ICAM1,ICAM2
Immune response	5.57E-04	AICDA,ANGPT2,APLN,ASS1,CASP4,CCL1, CD209,CD93,CIITA,CTF1,CXCL9,ELN,F7, FOXJ1,FYB,GJA1,GM2A,GZMA,HMGB1, HMGB1L1,HPGDS,ICAM1,IFI27L2,IFI44L, IL1RL1,Irgm2,LRP1(includes EG:16971), NOD2,PDE4B,SCGB1A1,SOCS1,SOCS2
Cell movement of dendritic cells	6.84E-04	CCL1,CD207,CD209,CXCL9,HMGB1, ICAM1,ICAM2
Migration of dendritic cells	7.23E-04	CD207,CD209,CXCL9,HMGB1,ICAM1, ICAM2
Cell movement of Langerhans cells	1.18E-03	CCL1,CD207,ICAM1
Cell movement of monocytes	1.56E-03	ANGPT2,CCL1,CXCL9,ELN,HMGB1,ICAM1, SOCS1
Cell movement of phagocytes	1.56E-03	ANGPT2,CCL1,CD207,CD209,CXCL9,ELN, HMGB1,HMGB1L1,ICAM1,ICAM2,IRGM, NOD2,PDE4B,SOCS1
Migration of phagocytes	1.87E-03	CCL1,CD207,CD209,CXCL9,HMGB1, HMGB1L1,ICAM1,ICAM2,PDE4B
Adhesion of phagocytes	2.70E-03	ANGPT2,CD209,HMGB1,ICAM1,ICAM2, IRGM
Activation of eosinophils	2.75E-03	CXCL9,HMGB1,IL1RL1
Chemotaxis of monocytes	3.03E-03	ANGPT2,CCL1,CXCL9,ELN,HMGB1
Aggregation of phagocytes	3.70E-03	CCL1,CD209,ICAM1
Recruitment of monocytes	4.05E-03	HMGB1,ICAM1,NOD2
Cell movement of macrophages	5.99E-03	ANGPT2,CXCL9,ELN,HMGB1,ICAM1,IRGM, SOCS1
Activation of mononuclear leukocytes	9.73E-03	AICDA,CD209,CD93,F7,FOXJ1,GZMA, HMGB1,ICAM1,IL1RL1,SOCS1,SOCS2
Aggregation of peritoneal macrophages	1.01E-02	CCL1
Contact growth inhibition of alveolar macrophages	1.01E-02	HMGB1
Contact growth inhibition of	1.01E-02	HMGB1

peritoneal macrophages		
Onset of transmigration of neutrophils	1.01E-02	ICAM1
Activation of leukocytes	1.10E-02	AICDA,CD209,CD93,CXCL9,F7,FOXJ1, GZMA,HMGB1,HMGB1L1,ICAM1,IL1RL1, LRP1 (includes EG:16971),SOCS1,SOCS2
Inflammation of secretory structure	1.25E-02	FOXJ1,SOCS1
Aggregation of antigen presenting cells	1.39E-02	CCL1,CD209
Migration of Langerhans cells	1.39E-02	CD207,ICAM1
Binding of macrophages	1.40E-02	CD209,HMGB1,ICAM1
Inflammatory response	1.41E-02	ANGPT2,CASP4,CCL1,CTF1,CXCL9,ELN, F7,HMGB1,ICAM1,IL1RL1,NOD2,PDE4B, SCGB1A1,SOCS1
Chemotaxis of myeloid cells	1.60E-02	ANGPT2,CCL1,CXCL9,ELN,HMGB1,NOD2, PDE4B
Inflammation of cells	1.63E-02	HMGB1,HMGB1L1,ICAM1,IL1RL1
Acute inflammatory response	1.71E-02	CTF1,HMGB1
Aggregation of myeloid cells	1.71E-02	CCL1,ICAM1
Infiltration by monocytes	1.71E-02	ANGPT2,SOCS1
Chemotaxis of phagocytes	1.86E-02	ANGPT2,CCL1,CXCL9,ELN,HMGB1,NOD2, PDE4B
Activation of peripheral blood leukocytes	1.88E-02	F7,SOCS1
Cell movement of bone marrow-derived macrophages	1.88E-02	HMGB1,IRGM
Quantity of neutrophils	1.92E-02	GJA1,HMGB1,ICAM1,PDE4B
Experimentally induced airway hyperresponsiveness of organism	2.01E-02	IL1RL1
Homing of endothelial progenitor cells	2.01E-02	IGFBP3

(**B**) Gene ontology category: Cellular Growth and Proliferation

Functions annotation	**p-Value**	**Molecules**
Proliferation of cells	7.39E-05	ADAMTS1,AICDA,ANGPT2,APLN,C8orf4, CAMK2A,CD209,CDH16,CHRNA1,CIITA, CREG1,CTF1,CXCL9,DLK1,ELN,EMP2, ESM1,F7,FGL2,FOXJ1,FYB,GJA1,Gm4617/ Ptma,HMGB1,HMGB1L1,HPGDS,ICAM1, IGFBP3,IL1RL1,INHBB,IRGM,JUN,LAMA4, LAMB1,LOX,LRP1 (includes EG:16971), MCC,Ms4a4b (includes others),NOD2,Prl2c2 (includes others), RCAN1,REG1A,RGS16, SCGB1A1,SERPINE2,SOCS1,SOCS2, TGFBI,TP53I11,TXLNA,WWOX,ZIC1
Proliferation of smooth muscle cells	2.80E-03	CTF1,ELN,F7,GJA1,HMGB1,IGFBP3,JUN, LRP1 (includes EG:16971)

Growth of fibroblasts	5.18E-03	CTF1,IGFBP3,JUN,SOCS1,TPM1 (includes EG:22003)
Proliferation of blood cells	8.32E-03	CD209,CHRNA1,CTF1,FGL2,FOXJ1,FYB, HMGB1,HPGDS,ICAM1, IL1RL1,IRGM, LOX, Ms4a4b (includes others),SCGB1A1, SOCS1, TXLNA
Formation of osteoclast-like cells	9.76E-03	ICAM1,TM7SF4
Generation of gamma-delta T lymphocytes	1.01E-02	JUN
Growth of cerebellar external germinal layer cells	1.01E-02	ZIC1
Inhibition of tumor-associated macrophages	1.01E-02	HMGB1
Proliferation of proepicardial cells	1.01E-02	GJA1
Stimulation of chronic lymphocytic leukemia cells	1.01E-02	TXLNA
Stimulation of prostate cancer cell lines	1.01E-02	IGFBP3
Proliferation of Th2 cells	1.11E-02	IL1RL1,SOCS1
Proliferation of T lymphocytes	1.24E-02	CD209,CHRNA1,FGL2,FOXJ1,FYB,HMGB1, ICAM1,IL1RL1,IRGM, Ms4a4b (includes others),SCGB1A1,SOCS1
Stimulation of cells	1.25E-02	ANGPT2,CD209,CHRNA1,FGD3,HMGB1, HMGB1L1,IGFBP3,TXLNA
Proliferation of lymphocytes	1.26E-02	CD209,CHRNA1,FGL2,FOXJ1,FYB,HMGB1, HPGDS,ICAM1,IL1RL1, IRGM,Ms4a4b (includes others),SCGB1A1,SOCS1,TXLNA
Growth of endocrine cells	1.71E-02	C8orf4,SOCS1
Proliferation of Schwann cells	1.71E-02	LAMA4,SERPINE2
Growth of thyroid cells	2.01E-02	C8orf4
Proliferation of adrenal glomerulosa cells	2.01E-02	ANGPT2
Proliferation of naive helper T cells	2.01E-02	ICAM1
Stimulation of adrenal glomerulosa cells	2.01E-02	ANGPT2
Stimulation of peripheral blood lymphocytes	2.01E-02	CHRNA1

Supplementary Table S3. List of qPCR primers

Gene	Species	Vendor
CA9	Human	5' CCCCAGAATAATGCCCACAGGGA-3'; 5'-GCCTAGGCTGGGGTATGGGAGG-3'; Integrated DNA Technologies Inc (IDT, CA)
Car9	Mouse	5'-CAGCTGCATGGCCTCCCTGG-3'; 5'-TCCCCCTGCATCCCGGACAG-3'; Integrated DNA Technologies Inc (IDT, CA)
H-2D^{d}	Mouse	Koch et al (2006) Immunol 119(1):98-115; Integrated DNA Technologies Inc (IDT, CA)
H-2K^{d}	Mouse	Koch et al (2006) Immunol 119(1):98-115; Integrated DNA Technologies Inc (IDT, CA)
Ccl1	Mouse	Applied Biosystems (AB, CA)
Cxcl9	Mouse	Applied Biosystems (AB, CA)
Hmgb1	Mouse	Applied Biosystems (AB, CA)
Fgl2	Mouse	Applied Biosystems (AB, CA)
Cd209a	Mouse	Applied Biosystems (AB, CA)
Foxj1	Mouse	Applied Biosystems (AB, CA)
Klra2	Mouse	Applied Biosystems (AB, CA)
miR-1186	Mouse	Applied Biosystems (AB, CA)
miR-98	Mouse	Applied Biosystems (AB, CA)
miR-5097	Mouse	Applied Biosystems (AB, CA)
miR-708	Mouse	Applied Biosystems (AB, CA)
miR-1942	Mouse	Applied Biosystems (AB, CA)
18s	Mouse	Applied Biosystems (AB, CA)
snoRNA234	Mouse	Applied Biosystems (AB, CA)
snoRNA202	Mouse	Applied Biosystems (AB, CA)

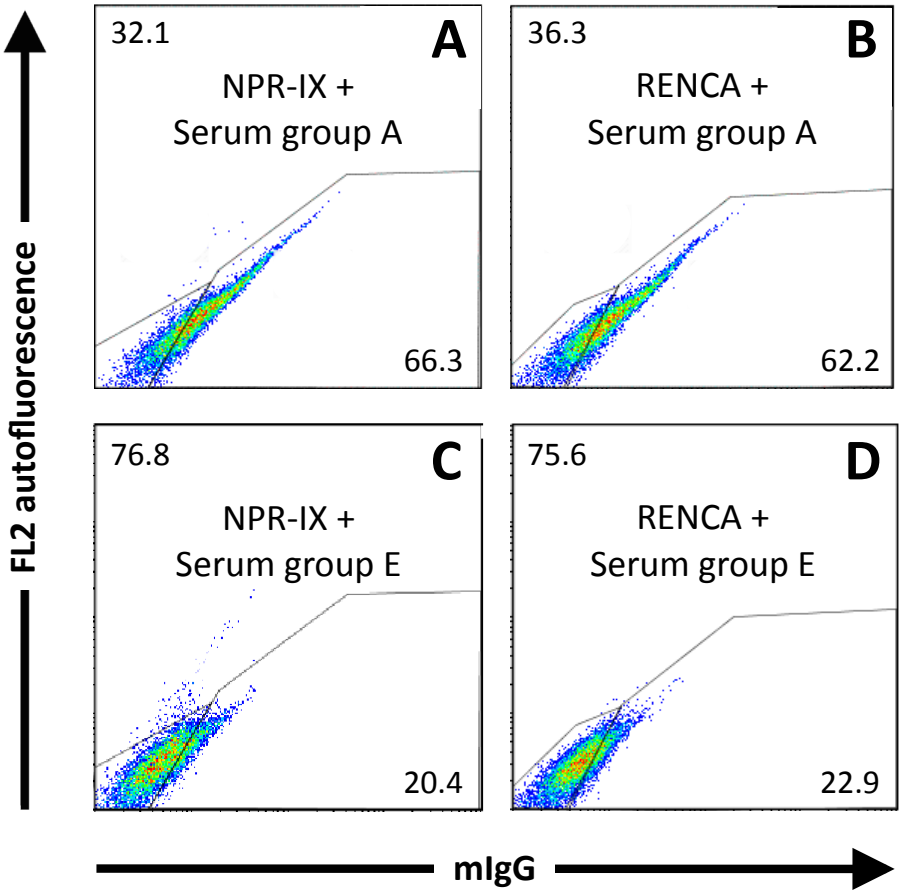

Supplementary Fig. S1. Dot plots of indirect FACS for anti-hCAIX antibodies using (**A**) NPR-IX and (**B**) RENCA stained by mouse serum from group A, and (**C**) NPR-IX and (**D**) RENCA stained by mouse serum from group E, followed by staining with FITC-conjugated anti-mouse IgG. Comparable rates of positive staining for mouse IgG within group A and group E suggest that sera of mice of group A and E do not contain measurable amounts of mouse anti-hCAIX antibodies.

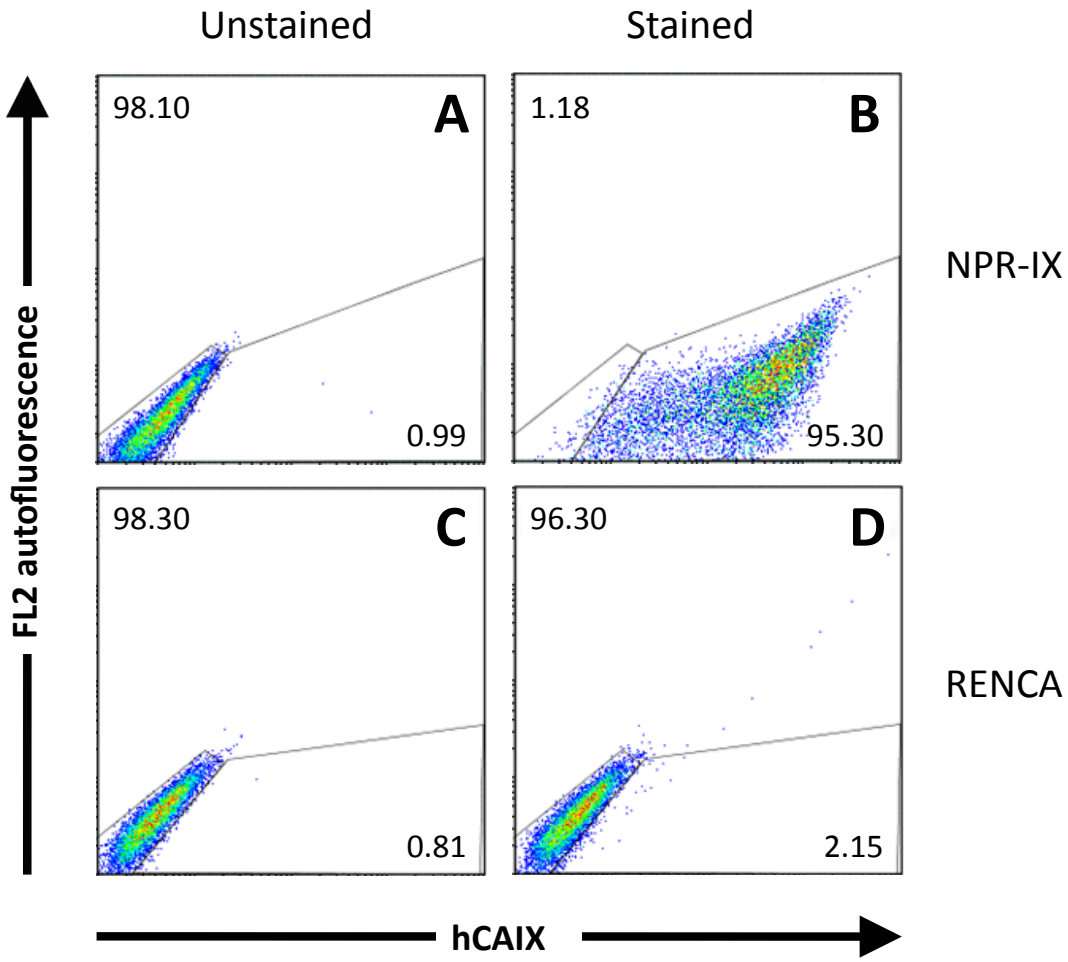

Supplementary Fig. S2. Dot plots of FACS for hCAIX in NPR-IX and RENCA cells. (**A**) Unstained NPR-IX; (**B**) NPR-IX stained with anti-hCAIX-FITC, showing 95.30% of cells positive for hCAIX expression; (**C**) Unstained RENCA; (**D**) RENCA stained with anti-hCAIX-FITC, showing 2.15% of cells positive for hCAIX expression, which is assumed to be an artifact of nonspecific binding.

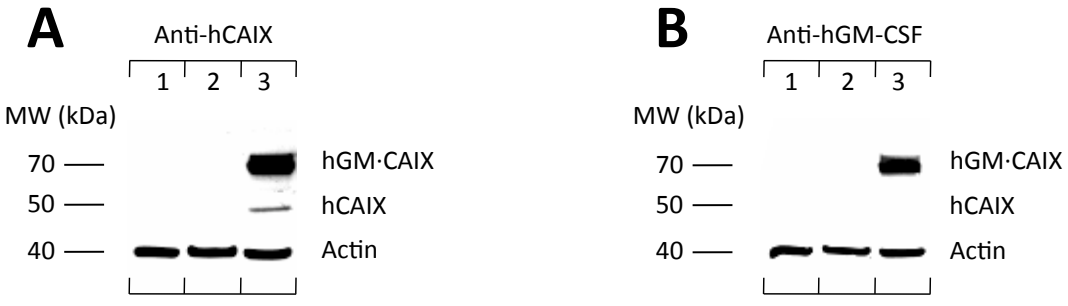

Supplementary Fig. S3. Western blot of the fusion protein hGMCAIX. The 70 kDa weight seen in both blots shows that the hGM·CAIX fusion gene is primarily expressed as a fused protein. Lane 1: 293T control; lane 2: 293T infected with Ad-Null; lane 3: 293T infected with Ad-GM·CAIX; (**A**) Gel exposed for actin loading control and hCAIX; (**B**) Gel exposed for actin loading control and hGM-CSF.

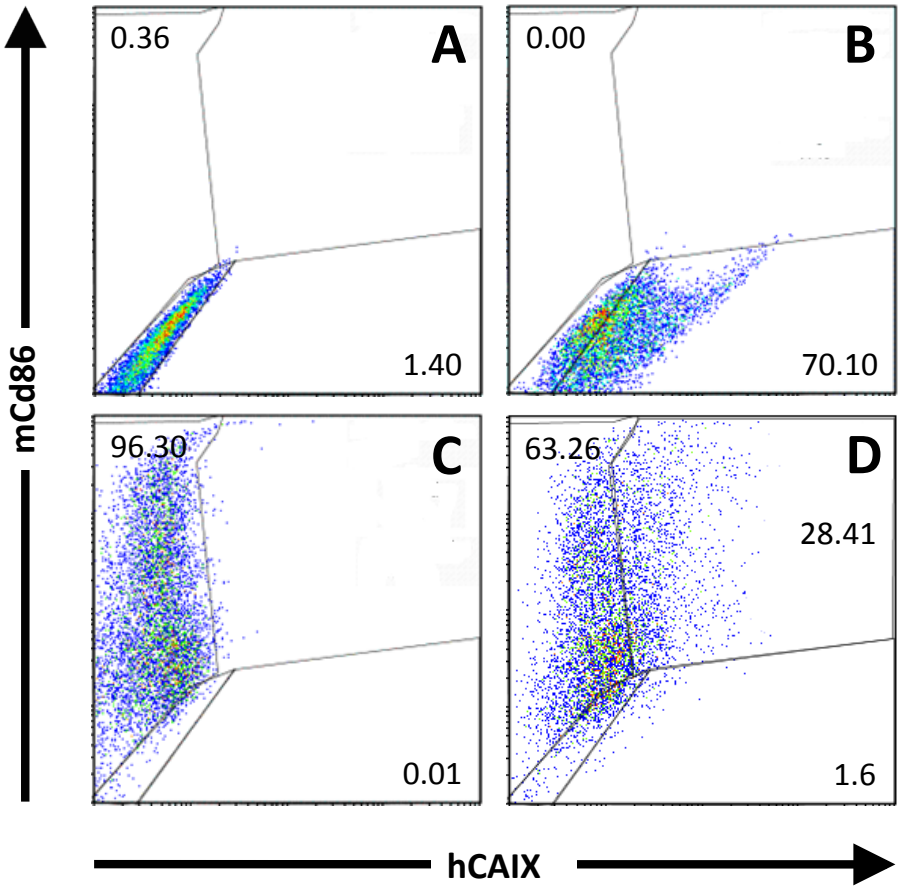

Supplementary Fig. S4. Dot plots of FACS for hCAIX (representative of hGM·CAIX expression) and mCd86 in DC-Ad-GM·CAIX; (**A**) Unstained DC-Ad-GM·CAIX; (**B**) DC-Ad-GM·CAIX stained with anti-hCAIX-FITC, showing 70.1% of cells positive for hCAIX expression, indicating successful infection of DCs with Ad-GM·CAIX; (**C**) DC-Ad-GM·CAIX stained with anti-mCd86-PE, showing 96.3% of cells positive for mCd86 expression, indicating successful differentiation from BMCs into DCs; (**D**) DC-Ad-GM·CAIX double-stained with anti-hCAIX-FITC and with anti-mCd86-PE, showing 28.4% of cells positive for both hCAIX and mCd86 expression, representing the percentage of hCAIX-expressing DCs.

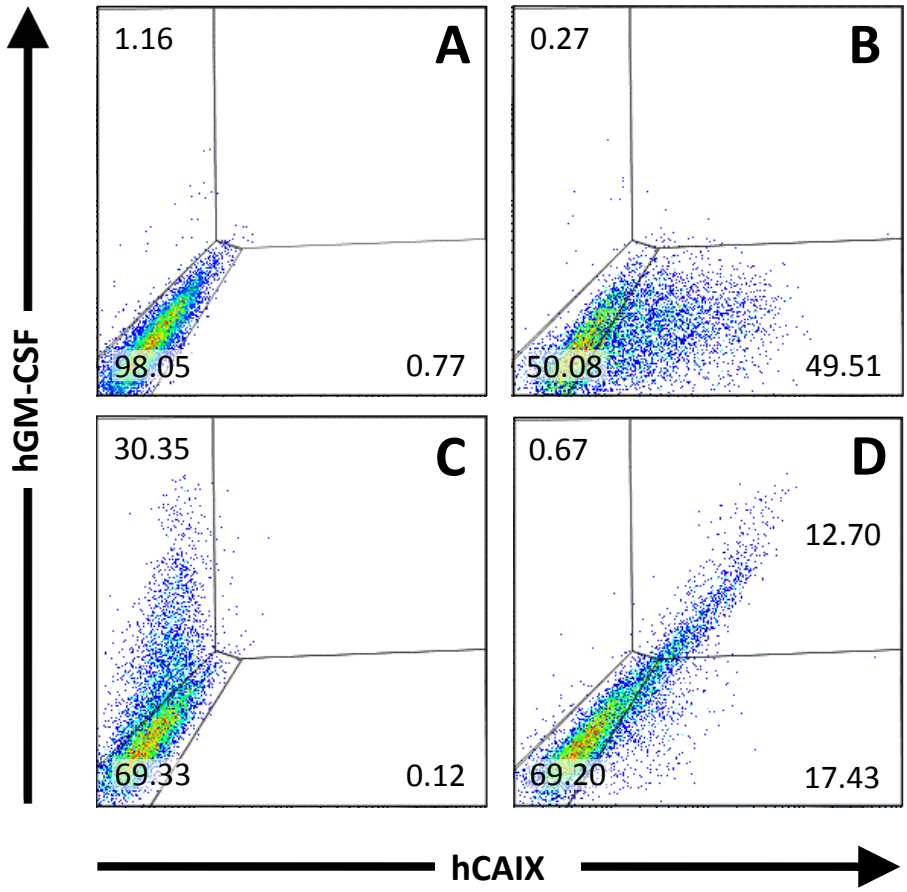

Supplementary Fig. S5. Dot plots of FACS for hCAIX and hGM-CSF expression in DC-Ad-GM·CAIX. (**A**) Unstained DC-Ad-GM·CAIX; (**B**) DC-Ad-GM·CAIX stained with anti-hCAIX-FITC, showing 49.51% of cells positive for hCAIX expression; (**C**) DC-Ad-GM·CAIX stained with anti-hGM-CSF-PerCP, showing 30.35% of cells positive for hGM-CSF expression; (**D**) DC-Ad-GM·CAIX double-stained with anti-hCAIX-FITC and anti-hGM-CSF-PerCP, showing 12.70% of cells positive for both hCAIX and hGM-CSF expression.